ODOR RESPONSE PROPERTIES OF NEIGHBORING MITRAL/TUFTED CELLS IN THE RAT OLFACTORY BULB

J. I. EGAÑA, M. L. AYLWIN AND P. E. MALDONADO*

Fisiologia y Biofisica, Facultad de Medicina, Universidad de Chile y Centro de Neurosciencias Integradas, ICM, Casilla 70005 Santiago 7, Chile

Abstract—Olfactory perception initiates in the nasal epithelium wherefrom olfactory receptor neurons—expressing the same receptor protein—project and converge in two different glomeruli within each olfactory bulb. Recent evidence suggests that glomeruli are isolated functional units, arranged in a chemotopic manner in the olfactory bulb. Exposure to odorants leads to the activation of specific populations of glomeruli. In rodents, about 25–50 mitral/tufted cells project their primary dendrites to a single glomerulus receiving similar sensory input. Yet, little is known about the properties of neighboring mitral/tufted cells connected to one or a few neighboring glomeruli. We used tetrodes to simultaneously record multiple single-unit activity in the mitral cell layer of anesthetized, freely breathing rats while exposed to mixtures of chemically related compounds. First, we characterized the odorant-induced modifications in firing rate of neighboring mitral/tufted cells and found that they do not share odorant response profiles. Individual units showed a long silent (11.01 ms) period with no oscillatory activity. Cross-correlation analysis between neighboring mitral/tufted cells revealed negligible synchronous activity among them. Finally, we show that respiratory-related temporal patterns are dissimilar among neighboring mitral/tufted cells and also that odorant stimulation results in an individual modification that is not necessarily shared by neighboring mitral/tufted cells. These results show that neighboring mitral/tufted cells frequently exhibit dissimilar response properties, which are not consistent with a precise chemotopic map at the mitral/tufted cell layer in the olfactory bulb.

Key words: olfactory bulb, mitral/tufted cells, tetrodes, synchrony, olfactory coding, respiratory modulation.

The mammalian olfactory system can discriminate among thousands of different chemical stimuli. This sensory ability is used to direct a broad range of behaviors that include the search for food, prey–predator recognition, path tracking and mating. In mammals, odorant molecules activate different sets of G-protein-coupled odorant receptors in the olfactory epithelium (Firestein, 2001). Each olfactory receptor neuron (ORN) expresses only one of the approximately 1000 members of the gene family of receptors (Buck and Axel, 1991). Axons of ORNs that express the same receptor converge in two glomeruli within the main olfactory bulb (OB) (Vassar et al., 1994; Mombaerts et al., 1996). A single odorant can activate several glomeruli (Rubin and Katz, 1999; Belluscio and Katz, 2001) and odorants with similar chemical structures activate glomeruli within certain regions of the OB, consistent with a chemotopic map at the glomerular layer of the OB (Uchida et al., 2000; Meister and Bonhoeffer, 2001; Inaki et al., 2002). Thus, odorants are represented in the OB as the differential activation of particular combinations of glomeruli (Rubin and Katz, 2001).

In mammals, the main output of the OB are the mitral/tufted (MT) cells whose primary dendrites project to a single glomerulus located externally to the soma (Macrides and Schneider, 1982; Mori et al., 1983). Histological studies have demonstrated that most of the mitral cells that innervate the same glomerulus are separated by less than 120 μm (Buonviso et al., 1991), indicating that MT cells that connect to a single glomeruli and receive similar sensory input are most likely neighbors within the mitral cell layer (Buck and Axel, 1991; Buonviso et al., 1991; Zou et al., 2001). Thus, MT cells connected to a single glomerulus may receive similar sensory input and thus share similar receptive field properties. However, MT cells receive additional inputs from other glomeruli through their secondary dendrites that travel as long as 1 mm within the OB (Mori et al., 1983; Orona et al., 1983). Furthermore, recurrent and lateral inhibition due to the mitral-granule-mitral loop could also modulate the odorant preference of MT cells (Jahr and Nicoll, 1980; Margrie et al., 2001; Xiong and Chen, 2002).

However, little is known about the functional organization of the MT cell layer. The assumption that neighboring MT cells exhibit similar receptive field properties has not been thoroughly tested. It can be argued that the receptive field properties of neighboring cells are determined by many different inputs that could influence or modify the direct sensory input to the glomerulus from the ORNs. Yet, there is limited evidence to support either view. In one study, Buonviso and Chaput, (1990) demonstrated that 95% of cells pairs recorded independently with two micropipettes separated by less than 40 μm, respond in a similar pattern when stimulated by an odorant. They also showed that neighboring cells exhibit similar respiratory induced firing patterns (Buonviso et al., 1992). More recent studies compared OB neurons located in the same cluster (Inaki et al., 2002) and have found that mitral and tufted cells exhibit differences in their responses to odorants (Nagayama et al., 2004). In summary, the question of the

*Corresponding author. Tel: +56-2-678-6035; fax: +56-2-777-6916.
E-mail address: pedro@neuro.med.uchile.cl (P. E. Maldonado).
Abbreviations: MT, mitral/tufted; OB, olfactory bulb; ORN, olfactory receptor neuron; POST, after-stimulus air exposure; PRE, pre-stimulus air exposure; STIM, stimulus delivery.

functional organization of the MT cells has not been elucidated.

In order to assess receptive field and temporal firing properties of neighboring MT cells, we employed the tetrode technique to precisely discriminate the activity of neighboring neurons (Gray et al., 1995; Buzsaki, 2004). We recorded single unit activity and respiratory cycle in freely breathing anesthetized rats during the stimulation with sets of chemically related mixtures of odorants. We compared the response profiles and temporal properties of simultaneously recorded neurons and we found that nearly all neighboring cell pairs differed significantly in their responses to odorants demonstrating a significant heterogeneity of neighboring MT cells.

EXPERIMENTAL PROCEDURES

Animals and surgical procedures

Surgical and experimental techniques were performed in accordance with institutional and the National Institutes of Health Guide for the Care and Use of Laboratory Animals (NIH Publications No. 80–23) revised 1996. All efforts were made to minimize the number of animals used and their suffering. Anesthesia was induced in adult male and female Sprague–Dawley rats (250–420 g) with a single i.p. injection of ketamine (70 mg/kg) and long lasting anesthesia was obtained using urethane (1–1.2 g/kg, i.p.). The leg withdrawal reflex in response to a moderately intense toe pinch was used to constantly monitoring the depth of anesthesia. Atropine (0.05 mg/kg, i.m.) was used to prevent an excess of respiratory secretions. Electrocardiogram and body temperature were monitored throughout the experiment, the latter was kept between 36 and 37 °C with a heating pad. To expose OBs, animals were positioned in a stereotaxic apparatus and a craniotomy was performed over the dorsal surface of these structures. Once the dura was removed with a small incision, electrodes were positioned over the OB and agar was applied to prevent dehydration and electrode bending. After the experiment animals were killed with an i.p. overdose of thiopental.

Electrophysiology

Single-unit activity was obtained using custom-made nichrome tetrodes (12 μm wire) 1–3 MΩ impedance at 1 kHz, see Gray et al. (1995) for details. Briefly, four plastic-coated wires were wound together and welded with a heat gun. The tetrode was cut and the tip rounded with a grinding wheel. The four ends of the wires were cold-soldered with conductive paint to a four-pin connector. Signals were amplified (10,000 times), bandpass filtered (300–5000 Hz) and digitized (27 kHz/channel) using PC custom designed software. Breathing was monitored using a thermocouple placed in front of the animal's nostrils and its signal was acquired at 100 Hz.

Odorant stimuli and delivery

Within the OB, glomeruli are organized in a chemotopic way; accordingly certain regions respond to specific molecular features like principal group and carbon chain length (Uchida et al., 2000; Meister and Bonhoeffer, 2001; Inaki et al., 2002). Consequently, we optimized the probability of response by using five different stimuli consisting in mixtures of chemically related compounds. Four of the mixtures consisted of chemically related compounds: alcohols (1-propanol, 1-butanol, 1-pentanol, 1-hexanol, 1-heptanol), carboxylic acids (propionic acid, butyric acid, pentanoic acid, hexanoic acid, heptanoic acid), aldehydes (propionaldehyde, butyraldeyhe, pentanal, hexanal, hepatanal) and ketones (2-hexanone, 3-hexanone). The fifth stimulus was a mixture of three unrelated compounds (*R*-(+)-carvone, *R*-(−)-carvone, isoamyl acetate). All chemicals of the mixtures (Sigma-Aldrich, St. Louis, MO, USA) were placed in their liquid form (highest purity available or diluted in mineral oil 1/100) in the same proportion. Stimuli were delivered by a computer-controlled custom-made olfactometer that allows a three l/min purified and humidified airflow to switch between an empty and stimulus filled plastic tubes. Airflow system ended in an inverted funnel in front of the animal's nose. Each trial consisted of 2 s of pre-stimulus air exposure (PRE), 4 s of stimulus delivery (STIM), and 4 s of after-stimulus air exposure (POST). Between trials, pure air was flowed through the olfactometer for at least 5 s. Typically, all five stimuli and pure air were presented between 10 and 25 times at each recording site.

Spike sorting

The tetrode allows the detection of action potentials from four different recording wires (Fig. 1A). The resulting signals were processed with an off-line sorting program to reconstruct the spike trains. For each of the different data sets, spike separation was achieved by an interactive custom computer program (Maldonado and Gray, 1996). In this program, selected spike parameters for any two of the four recording channels of the tetrode are displayed in two dimensional scatter plots, revealing a clustering of values. Once a unique cluster is defined as a single cell, the spike train of each cell is computed by recovering the time stamp of each data point in the cluster. The extracted spike train for each cell was stored with a 0.1 ms resolution.

Data analysis

For each epoch (PRE, STIM and POST) raster plots, instantaneous firing rates, autocorrelograms, crosscorrelograms and peristimulus time histograms (PSTH) were computed using MATLAB (MathWorks, Natick, MA, USA) and LabWindows CVI (National Instruments, Austin, TX, USA) software. We considered an excitatory or inhibitory response in the STIM or POST epochs when the average value of the firing rate exceeded or fell below the significance levels computed for the PRE epoch. This significance level was determined by the mean plus (or minus) two times the standard deviation of the firing rate at the PRE epoch. In order to compare the similarity of responses of neighboring MT cells, we computed the response ratios between the mean firing rates during each epoch using the following equation:

$$\left(\frac{X_S}{X_A}-1\right) \text{ if } \frac{X_S}{X_A}\geq 1 \text{ or } \left(\frac{-1}{X_S/X_A}\right)+1 \text{ if } \frac{X_S}{X_A}<1 \qquad (1)$$

Where X_S is the STIM or POST mean firing rate and X_A the PRE mean firing rate. For example, if a cell significantly duplicates its firing rate, the corresponding response ratio will be 1, and if significantly decrease it rate by half the ratio will be −1. We then built 2D scatter plots in which each point represents the response ratios of a pair of neighboring neurons (X and Y) in which at least one of them showed a significant response during STIM or POST. This way we can directly compare the response ratio for a large population of cells by comparing the distributions of points to a linear diagonal expected if both cells of each pair exhibit similar response properties.

Because temporal properties of the olfactory neurons are thought to be instrumental in olfactory coding (Laurent, 1999), we examined the neuronal rhythmicity of neighboring MT cells by calculating the power spectrum of each autocorrelogram (±128 ms time lag) and extracted the frequency and amplitude of the peak value in the frequency range of 20–80 Hz (Gray and Viana, 1997). The statistical significance of the spectral peaks was estimated using a Monte Carlo simulation. For this procedure, we generated an equivalent pseudo-random spike train for each win-

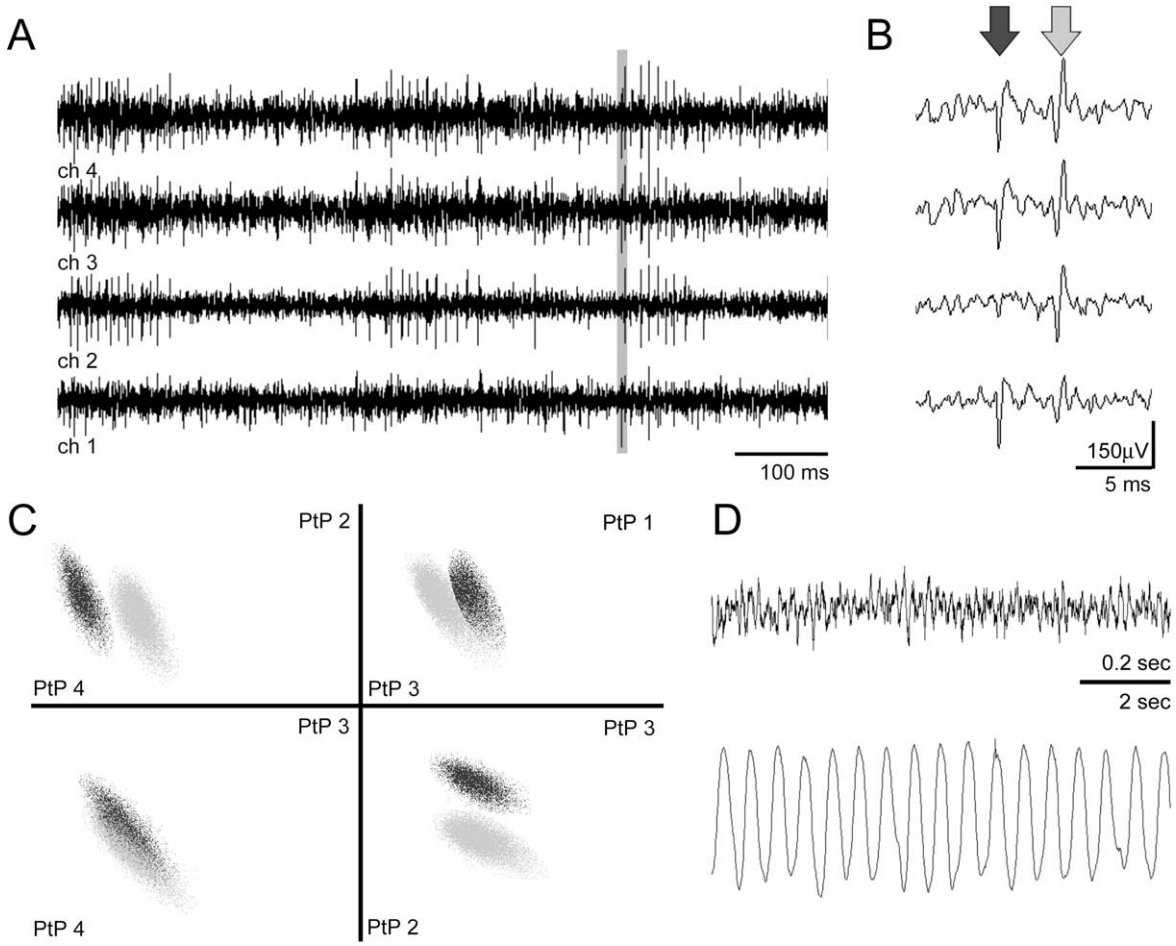

Fig. 1. Example of a tetrode recording in the MCL. (A) Traces showing raw data recorded with the four wires of a tetrode. Extracellular action potentials of neurons located nearby the tip of the electrode display different amplitudes depending on their spatial distribution. (B) Magnification of shaded zone of A. The arrows show two different neurons with unique representations across the four channels. (C) Each neuron's spike forms clusters in 2D plots that can be followed through the parameter space to be uniquely identified. Here, four peak-to-peak spike amplitude plots from different wire combinations. (D) The upper plot shows 1 s of local field potential signal extracted from channel 1. Lower plot shows 10-s respiration signal recorded with a temperature probe adjoining the nostril.

dow of data collected on each trial using a random sample from a uniform distribution and a silent period identical to the data. The autocorrelogram and corresponding power spectrum were computed for each simulated data set and the peak value in the spectrum between 20 and 80 Hz was extracted. The simulation was repeated 500 times and any experimental value was considered significant if it was greater than the largest simulated value ("cutoff"). The ratio of the experimental peak to the simulated cutoff served as a measure of oscillation strength or amplitude (Friedman-Hill et al., 2000). Similarly, synchronous activity among neighboring MT cells was assessed comparing each central area of the crosscorrelogram to an equivalent pseudo-random cross-correlogram obtained from simulated spike trains with identical spike counts, mean firing rate and duration to the experimental data. For both calculations the simulation was repeated 500 times and any experimental value was considered significant if it was greater than the 99% of simulated value or cutoff value (Maldonado et al., 2000).

Since the MT cells firing rate exhibits a modulation by the respiratory cycle (Chaput, 1986; Buonviso et al., 1992, 2003) we computed PSTHs using the central time of the inhaling phase of the respiratory cycle as reference. We considered the average respiratory signal as a single sine wave, where 90° correspond to the end of exhalation and 270° to the end of inhalation. These cycle-based PSTHs (20 ms bin) were constructed for each cell and significant peaks and/or troughs (mean±2 S.D. from baseline) were assigned to one of the four divisions of the cycle (90, 180, 270 or 360°) according to their location in the respiratory cycle.

RESULTS

We recorded 261 units from 103 sites in 25 animals. Penetrations were done all over the dorsal surface of both OBs and recordings were obtained from both dorsal and ventral mitral cells layers. Between one and six (mean=2.5) cells were acquired at each site. The aim of this study was to characterize response properties of neighboring MT cells, thus multi-unit recordings, or recordings containing a single cell or a cell with very low spike count (<0.5 Hz) were not included in this analysis.

We analyzed 70 single units in 29 sites of 11 rats, with a mean of 2.4 cells per site. In previous studies using the same recording technique we demonstrated that only MT

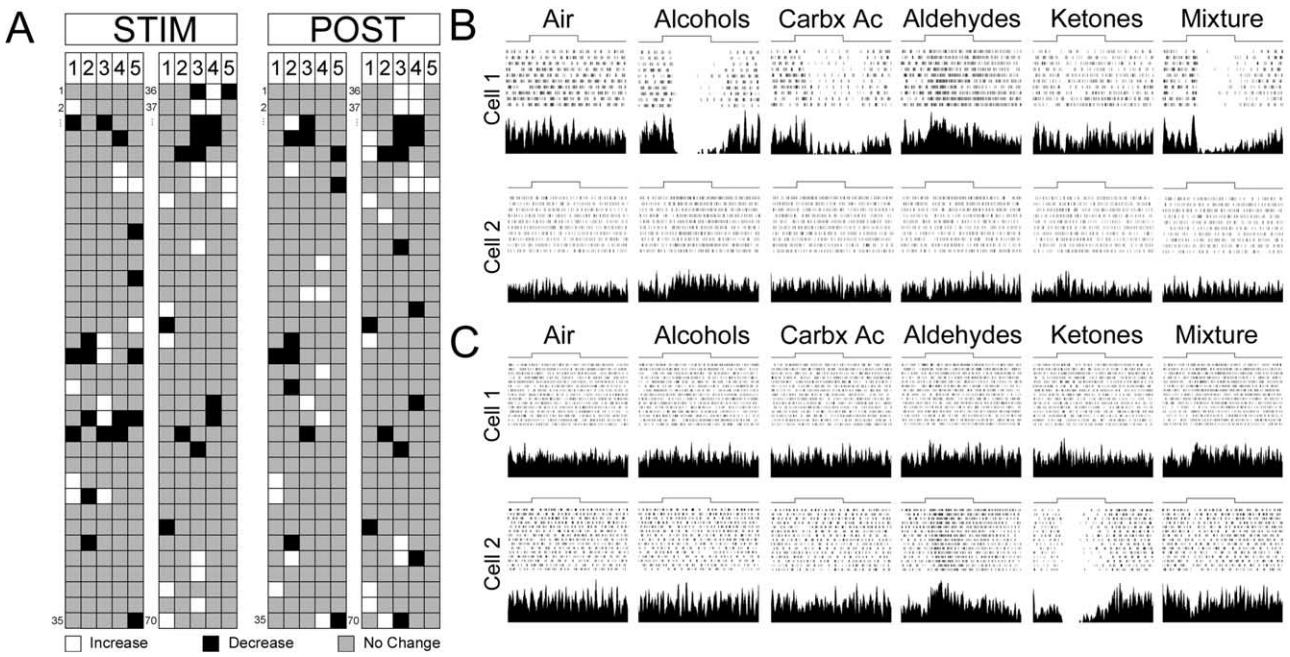

Fig. 2. Summary and examples of neighboring MT cells responses. (A) Two-dimensional matrix that shows the activity of the 70 recorded cells for both STIM and POST. Some cells exhibits opposite behaviors for different odorants. (B) Example of responses to different stimuli by two neighboring MT neurons. Rasters for 15 odor presentations are shown in the upper panel while instantaneous firing rates (IFR) are shown in lower panel (bin size 50 ms). The line above the rasters represents stimulation protocol. Cell 1 is inhibited by alcohols, carboxylic acids and the mixture and excited by aldehydes and ketones. Cell 2, in turn, is only excited by alcohols and ketones with no other response found for the other stimuli. (C) Neighboring MT cells could show the same behavior to some odorants (both are excited by aldehydes) and opposite for others (ketones). Note that cell two exhibit a clear post-stimulus increase in firing rate after ketones exposure.

cells are large enough to be recorded with this electrode. In addition, histological procedures showed that electrolytic lesions were found only in the mitral cell layer (Aylwin et al., in press). In addition, the depth of recordings and the OB electrophysiological characteristics made the mitral cell layer relatively easy to distinguish, as demonstrated by Kay and Laurent (1999) using a similar technique. Fig. 1A shows an example of MT cells activity as recorded by the four channels of the tetrode. Each cell shows a unique profile of spike amplitudes corresponding to each of the four wires. An expansion of the shaded segment in 1A (Fig. 1B) shows that there are clear differences in spike amplitude on neighboring channels and the ratios of these differences vary from cell to cell. The spike amplitude along with waveform profiles and principal component analysis was used to build 2D-scatter plots and sort single unit activity (Fig. 1C). Local field potentials and respiration signals were also recorded during each stimulus presentation. Fig. 1D shows the respiratory signal associated to the epoch shown in 1A.

M/T cells responses to odorant mixtures

We found that MT cells show a broad range of spontaneous activity ranging from 5.5–191.7 Hz (60±41 Hz, mean±S.D.). To compare the response profile of neighboring cells pairs, we selected those recordings in which at least one of the cells from the cell pair responded (whether excitatory or inhibitory) to one or more olfactory stimulus. These consisted in two to five odorants with the same main chemical group but with different carbon chain length (see Experimental Procedures). We found that in addition to changes in firing rate during the exposure to the odorant stimulus (STIM), many cells also exhibited rate modulations during stimulus offset (POST). In summary, 47 of 70 cells (67.1%) showed significant changes (increase or decrease) in their average firing rate during (STIM) or immediately after (POST) odorant presentation with at least one of the five-odorant mixtures. Although a few MT cells show complex response profiles, the majority of cells recorded exhibited sustained responses during the STIM and POST epochs, despite respiratory modulation.

When we examined the MT cells firing rate responses to the different odorant mixtures, we found that from a population of 70 cells, 22 (31%) responded to one odorant mixture, 11 (16%) responded to two of the mixtures and 14 (20%) to three or more of the mixtures. A summary of the responses from all cells to each odorant mixture is shown in Fig. 2A.

Stimuli evoked different responses among neighboring M/T cells

From the 70 single units recorded, we obtained 58 pairs of simultaneously recorded neighboring MT cells. From these, only eight pairs showed no modification in firing rate for any of the stimulus in the set. The remaining 50-cell pairs exhibited a dissimilar response (increase, decrease or no change) to at least one of the stimuli. Most of the differences observed in the responses of the cells these

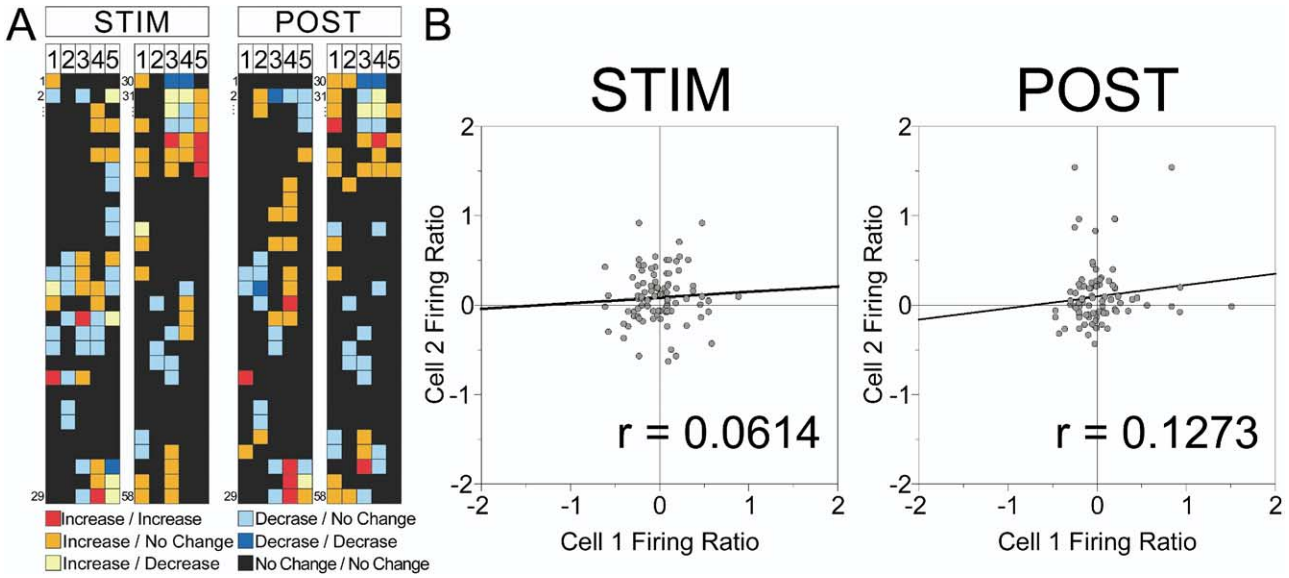

Fig. 3. Neighboring MT cells typically exhibit different odorant preferences. (A) Two-dimensional matrix that shows the activity of 58 pairs of MT cells recorded for both STIM and POST. Most pairs of cells exhibit individual responses to odorants (see code below) while the other cell showed no response (black). Most cell pair differs in their response to at least one stimulus condition. (B) Two-dimensional plots in which each axis represents the firing rate ratio between stimulus and air for each neighboring cell pair. Each point represents cell pair in which at least one of them changes significantly its firing rate. If both cells of each pair exhibit similar response to odorants, the points should lie close to a diagonal line. A linear regression of points reveals a near flat slope (r=0.06). (C) A similar analysis for firing rate ratio between POST and AIR also shows a deviation from a diagonal (r=0.12) indicating that neighboring cells frequently do not co-vary their firing rate during odorant stimulation.

pairs relate to their odorant preference rather than on the magnitude of the excitatory and/or inhibitory responses. When we examined the response patterns of different cells pairs across all five stimuli we found that the majority of the cell pairs showed similar preferences to at least two of the mixtures, but they differed in their responses to at least one stimulus of the set. In Fig. 2B, rasters and instantaneous firing rates show the odor preference profile for two neighboring cells. Cell 1 responded with a strong inhibition to alcohols, carboxylic acids and the dissimilar compounds while it was strongly excited by aldehydes and lightly excited by ketones. Alcohols and ketones, in turn, only weakly excited cell 2, with no other response found for the other stimuli. An example of two cells of a pair responding with an increase in firing rate to aldehydes while the opposite behavior was found for ketones is shown in Fig. 2C. Surprisingly, we did not find cell pairs that exhibited similar onset and offset stimulus responses to the complete set of stimuli. In Fig. 3A we show a summary graph for all cell pairs, where a color code indicates the type of response of both cells of the each pair to the entire stimulus set. Because of the large set of parameters on which the responses could be compared, we devised a simple measure to quantify the similarity of the response of neighboring cells by comparing the relative changes in firing rate for each cell of a neuronal pair (Fig. 3B). Each axis represents the magnitude of the firing rate modification (positive if it is an increase, negative for decrease) for each of the two cells (see Experimental Procedures). If the firing rate changes for a given stimulus is similar for both cells of a pair, that point should fall close to a diagonal line going from the lower left to the upper right quadrants of the graph. On the other hand, if cell pairs exhibit completely independent responses, the points will be randomly distributed in all quadrants. Thus, a large degree of similarity in the responses of neighboring neurons would result in a significant linear correlation with a slope of 1.0. In this analysis, we included each cell pair for all five stimuli, but excluded those points where both cells did not exhibit a significant response to that particular stimulus. Fig. 3B shows the computation of response rations of 94 cells pairs between odorant stimulation (STIM) and air (PRE). A linear regression of this data yields a coefficient of 0.06. Similarly, in Fig. 3C, we included 86 pairs comparing the ratio of responses between POST and PRE, which show a regression coefficient of 0.12. This result indicates that during stimulus response as well as after stimulus offset, the response of neighboring MT cells differs significantly, demonstrating a large degree of heterogeneity of neighboring cells in the OB.

Silent period changes during odorant stimulation

In a previous study we found that MT cells exhibit an uncharacteristically long silent period between spikes that we referred to as silent or “refractory” period (Aylwin et al., in press). These silent periods ranged between 5 and 29 ms and were evident in the autocorrelogram histograms as well as in inter-stimulus time histograms. Indeed in our data we found that single unit spike trains with a small or no silent period were uncommon. Here we examined if this silent period changed during the odorant stimulation and whether neighboring cells show similar modifications of this silent period in the presence of odorants. We found

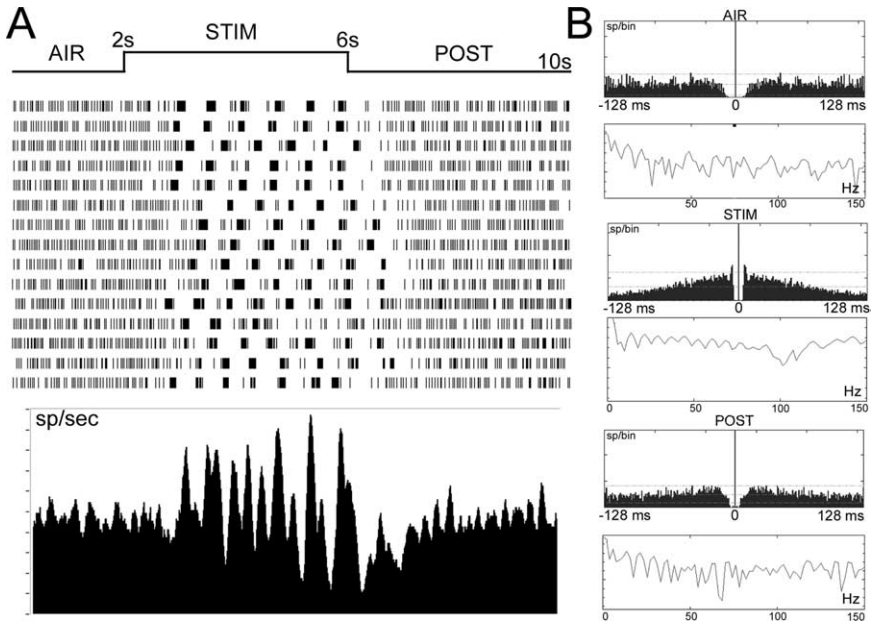

Fig. 4. MT Cells have a long silent period and low oscillation levels. (A) Raster and instantaneous firing rates for a mitral cell while exposed to an aldehydes mixture. Note the clear excitatory response during stimulus presentation. (B) Autocorrelogram and its power spectrums during PRE, STIM and POST. Note the long silent period during PRE (14 ms) that is shortened during STIM (10 ms) and partially recover during POST (12 ms). Power spectrums reveal no significant frequency.

that of 70 cells exposed to four or five stimuli, the responses showed a significant decrement on the silent period from an average of 11.0±7.3 ms to 9.9±6.7 ms ($P<0.01$, paired *t*-test). We also found a significantly shorter silent period of 10.0±6.3 ms during the POST stimulus stage. Fig. 4B shows an example of a cell with a 14 ms silent period during PRE. In the STIM epoch this period was reduced to 10 ms and then partially recovered after the stimulus (POST). For all pairs where both cells responded to a given stimulus we examined if one, both or none of the cells changed its silent period. We examined 23 cell pairs in which the two neurons exhibited the same type of response (excitatory or inhibitory) to the same odorant. In 13 pairs (56.5%) both cells decrease or increase their silent period, while in five pairs (21.7%) only one of them changed it, and in the remaining five pairs, we observed an increase in the silent period of one cell of the pair and a decrease in the other.

Oscillatory and synchronous activity among neighboring MT cells

A remarkable feature of the neuronal activity in the OB is the robust oscillatory activity seen in the local field potential in the presence of odorants (Laurent, 1996; Buonviso et al., 2003; Ravel et al., 2003). We recorded the local field potential and found extensive field oscillations in the beta and gamma bands (Fig. 1). To determine whether MT single units within the OB exhibited oscillatory activity in the gamma frequency range (30–100 Hz) and whether this behavior was similar in neighboring cells, we computed the autocorrelogram for each cell. We found that none of the cells exhibited autocorrelograms with a significant oscillatory activity during PRE, while only 0.7% of the cells showed oscillatory activity during STIM and 1.7% during POST. In summary, we found a very low occurrence of significant sustained oscillatory activity at the single unit.

Even if MT cells do not show oscillatory activity, nearby neurons could exhibit coherent (synchronous) activity due to the common sensory input received through the glomerulus (Schoppa and Westbrook, 2002). To test this hypothesis, we examined the incidence of correlated firing among neighboring MT cells recorded with the same electrode. We computed the crosscorrelograms for 58 cell pairs for all stimuli and found very low incidence (0.31%) of synchronous firing among neighboring cells during PRE. During STIM we found a small increase in the incidence of synchronous discharge (2.80%) and a slight increased during POST (3.78%). A typical example is shown in Fig. 5. A cell pair that responded to odorant stimulation shows no evidence of oscillatory or correlated activity.

Respiratory patterning in MT cells

MT cell firing is non-stationary both in the absence or presence of odorants. Many cells appear to be modulated by respiration, known as respiratory patterning (Chalansonnet and Chaput, 1998; Buonviso et al., 2003). MT cells could fire at different phases of the respiratory cycle and thus we aimed to determine whether neighboring cells share this property. We computed peristimulus time histograms using the center point of the inhaling phase as time reference and determined phase preferences in firing for 70 cells (see Experimental Procedures). We divided the respiratory cycle on four 90° epochs and found that during exposure to clean air, 41.4% (29/70) of the cells showed significant firing differences during one part of the cell cycle. We also found that 37.1% (26/70) of cells exhibit a

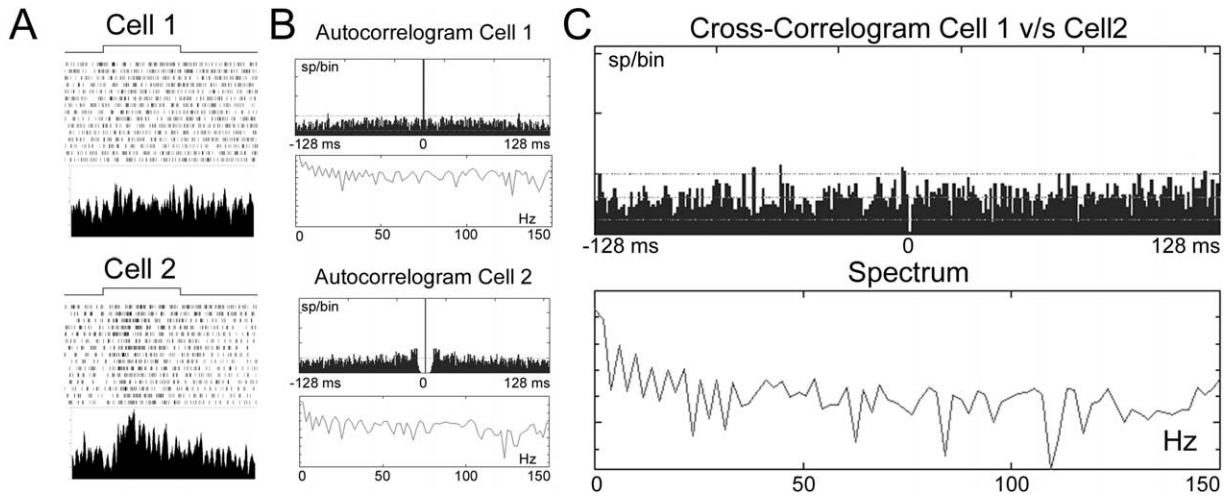

Fig. 5. Neighboring MT cells show low incidence of synchronous activity. (A) Raster and PSTSH of both cells, showing increased activity to the aldehydes. (B) Autocorrelograms and power spectrum for both cells showing no oscillatory activity. (C) Crosscorrelogram showing absence of significant peaks. At 0 time lag, there is absence of counts because these cells were extracted from the same tetrode. The power spectrum of this correlogram (below) shows that this correlogram lack oscillatory activity. Note that cell one lacks silent period.

phase shift or show bimodal distribution of their spike rate, when exposed to odorant stimuli. Fig. 6 shows an example of three simultaneously recorded cells whose activity, when exposed to air, is concentrated during different phases of the respiratory cycle. Cell M2 responds preferentially during the initial part of the inhaling phase, while cell M3 exhibits opposite behavior. Cell M1 shows little modulation with respiration, although some suppression occurs for aldehydes, ketones and the mixture during the end of exhalation. We observed that odorant stimulation modulates phase preferences. Cell M2 shifts cycle preference, from end of inhalation to end of exhalation, when exposed to aldehydes, ketones and the mixture. Cell M3 shows no modulation to any of these odorants.

When we compared the phase preference of neighboring MT cells during PRE, we found that 10.3% (6/58) of cell pairs show respiratory cycle phase preferences in both cells, 32.7% (19/58) show preference in one cell of the pair, and the reminder 56.9% (33/58) show no preferences in either cell. Of the six cell pairs where both neurons exhibited modulation, only two (33.3%) show modulation in the same phase of the cycle. These results show that neighboring cells may exhibit a heterogeneous response patterning during the respiratory cycle.

DISCUSSION

The aim of this study was to characterize the response properties of populations of neighboring MT cells in the OB. We used the tetrode's ability to record simultaneously many neighboring neurons. Several criteria were used to describe single cell profiles and cell pairs' behavior to different sets of chemically related (same principal group) compounds in anesthetized freely breathing rats. Here we show that neighboring MT cells do not necessarily have similar receptive properties to the molecular determinants of odorants or its main functional group. Little oscillatory activity was found among MT cells and synchronous firing occurred very rarely among neighboring output neurons. Finally we show that each cell has a particular firing pattern locked to the respiration cycle and this is individually modified by odorant stimulation. These findings suggests that the chemotopical organization found at the glomerular level of the OB (Uchida et al., 2000; Inaki et al., 2002; Uchida and Mainen, 2003) is not automatically extended at the MT cell layer, indicating that the OB is not a simple relay for the olfactory sensory input. The fact that odorant preferences along with precise firing and respiratory patterns behave independently for neighboring neurons indicates that olfactory processing within the OB is far more complex than previously thought and that ORN inputs to MT cells are substantially modified by other components of the OB circuitry.

Neighboring MT cells connections and odor preferences

In mammals, MT cells have a single primary dendrite that receives sensory inputs from only one glomerulus (Kishi et al., 1984). In turn, each of the glomeruli represent the activation of a single odorant receptor type (Ressler et al., 1994; Mombaerts et al., 1996; Buck, 2000). Histological studies using horseradish peroxidase labeling have demonstrated that 96% of the mitral cells innervating the same glomerulus are separated by less than 120 μm, this number decreased to 72% for cells connected to adjacent glomeruli. Furthermore, only 29% of the cells separated by 120 μM were connected to distant glomeruli (Buck and Axel, 1991; Buonviso et al., 1991). More recent studies using genetic approaches have confirmed that MT cells, that send their primary dendrite to a single glomerulus, are located within 120–160 μm (Zou et al., 2001). Since tetrodes have an estimated 65 μm detection radius (Gray et al., 1995), we postulate that neighboring MT cells, like the ones recorded in these experiments, have a high proba-

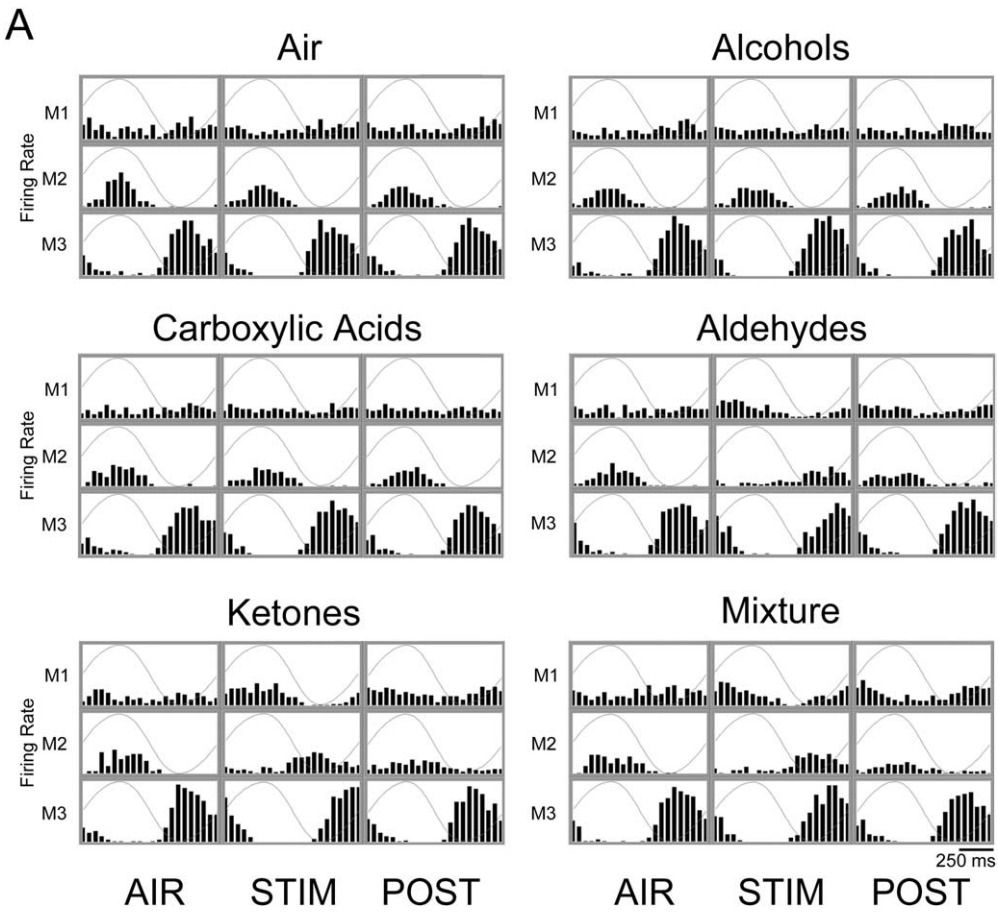

Fig. 6. Neighboring MT cells show different respiratory patterning. Respiratory cycle-based PSTH were built for each for an average of 15–25 stimulus presentation. The solid line represent the mean respiratory cycle where the upward and downward strokes denote the exhalation and inhalation phases, respectively. In this example, the activity of cells M2 and M3 is concentrated during opposite phases of the respiratory cycle. Aldehydes, ketones and mixture (STIM) induce a phase-shift in firing of M2 while evoke an end-of-inspiration inhibition in M1. Cell M3 is not affected by any stimulus.

bility of being connected to the same glomerulus or at least to be connected to adjacent glomeruli.

On the other hand, several groups have shown that glomeruli responsive to certain chemicals groups are clustered together covering broad areas of the OB surface (Johnson et al., 1998, 2002; Uchida et al., 2000; Johnson and Leon, 2000). Therefore, the OB areas responding to molecular determinants of odorants are located in clusters and thus will be activated with different strengths by chemically related odorants. Considering the anatomical connectivity of MT cells and the distribution of glomeruli responses, neighboring MT cells are very likely receiving the same or similar sensory input from adjacent glomeruli. Therefore, the fact that in most recordings we found MT cells responding to odorants that belong to well-separated glomeruli clusters (see cells in Fig. 2B, 2C), strongly suggests that MT cells are not a simple relay to the sensory signals from the ORN. Although there is evidence obtained from OB slices where only 27% of cells recorded are connected to the same glomerulus, with an additional 31% of cells connected to adjacent glomeruli (Schoppa and Westbrook, 2001), the great extent of the glomeruli clusters responding to the same chemical group makes improbable the recording of MT cells connected to glomeruli that belong to clusters with preferences to different chemical group.

A stimulation with a single chemical compound, will activate a particular combination of glomeruli that will in turn, define specific interactions through the periglomerular cells. Since periglomerular cells mediate interactions between adjacent and neighboring glomeruli, it could be argued that the use of odorant mixtures can modify glomeruli receptive properties. When a mixture of chemicals is used, a qualitatively similar but more complex set of periglomerular interactions given by the activation of additional glomerulus from the cluster will very likely induce reciprocal inhibitions between activated glomeruli compared with a single odorant stimulus situation. Although, we cannot rule out the possibility that glomerulus–glomerulus interactions modify the receptive properties at the glomerular layer, these interactions are mainly inhibitory (Aungst et al., 2003) and thus, could account for the large inhibitory response found (see Fig. 3A) but not for the fact that most of MT cells pairs exhibited responses to odorants that are supposedly encoded by distant glomeruli to the ones to which they connect. In most cases, a glomeruli cluster

responding to a particular chemical determinant common in each mixture, is clearly separated and does not overlap with the cluster corresponding to another chemical determinant (Uchida et al., 2000; Nagayama et al., 2004). In the same line of thought, the extension of these clusters makes very unlikely that different response profiles from neighboring MT cells in our data were due to the localization of the recordings in the boundary between clusters.

Our data suggest that the spatial pattern of odorant evoked activity in the sensory layer (ORN) is substantially transformed within the OB and that MT cells responses to ORN inputs are strongly modulated by other components. It has been previously shown that mechanisms such as recurrent and lateral inhibition can modify nearby neuronal firing (Schoppa et al., 1998). It is known, for example, that action potentials travel long distances (larger than clusters) within secondary dendrites (Christie and Westbrook, 2003) and that MT cells make numerous reciprocal synapses with granular cells in these dendrites (Shipley and Ennis, 1996). In vertebrates exposures to binary mixtures of odorants have revealed that the glomerular representation is far more predictable than the MT cells' response to the same stimulus(Tabor et al., 2004). This not so linear response of MT cells probably arises from interactions such as lateral inhibition. This mechanism acts distantly and could, for example, increase gain of weaker stimuli resulting in a broader spectrum of MT cells such as the ones observed in our data.

Previous studies in mammalian and non-mammalian models revealed that MT cells within certain areas share odorant preferences. Most of these studies were performed using single-cell recording so neither temporal (simultaneous recording) nor spatial (proximity of the cells) variables could be used to compare neighboring cell responses. The ability of tetrodes to simultaneously record several neurons that are close to the electrode's tip enables us to unambiguously assess the temporal properties of the responses of neighboring cells. In addition, artificial breathing was used in several cases, a procedure that may have altered MT cells' spontaneous activity. For instance, basal neuronal activity in artificial breathing experiments is almost nonexistent (see Mori et al., 1992, Fig. 1) while in our data, all MT cells revealed some degree of spontaneous activity. Experiments in behaving rats shows that certain level of activity is a strong feature in non-stimulated MT cells (Kay and Laurent, 1999). However, a single study reported that pairs of closely located cells (<40 μm) displayed similar response profiles to several odorants (Buonviso and Chaput, 1990). While Buonviso and Chaput (1990 used single odorants our stimulation protocol used mixtures of chemically related compounds at higher concentrations. It may have also contributed the recruitment that occurs when more than one odorant is present, and especially when high concentrations are applied (Johnson and Leon, 2000; Fried et al., 2002). In this case, the activity within the OB could lead to increasing differential activity in the MT cells. This expands the coding space features enabling to increase differences among very similar compounds (Friedrich and Laurent, 2001; Laurent, 2002). Although research is needed in order to clarify the relative contribution of the different inputs to a MT cell, our data indicates that ORN inputs are strongly modulated by the network in which each neuron is immersed.

Neighboring MT cells response profiles

To our knowledge, besides the Buonviso and Chaput (1990) report, this is the only study investigating the response properties of neighboring MT cells. In summary, we found that the majority of cell pairs exhibit differences in the odorant preference and type of response (excitation/inhibition). It can be argued that these differences reflect the two distinct classes of output neurons in the OB. Recent evidence indicates that mitral and tufted cells separated by more than 120 μm have different decoding attributes (Nagayama et al., 2004) revealed by the differences in the firing patterns (excitation/inhibition) more than their selectivity to the chemical nature of the stimulus, suggesting that our results could be explained by the inability to distinguish mitral from tufted cells. Our recording technique does not allow us to distinguish between the mitral and tufted cells, however, the number of mitral cells is higher than the tufted cells indicating that our results are not consistent with this ratio. This contrasts with our data where neighboring cells differ mostly in that feature. This is consistent with the hypothesis that sensory inputs to MT cells are transformed within the OB (Schoppa and Urban, 2003), giving place to a representation where MT cells are individual functional units with its own pattern of responses and molecular receptive range. One consequence this hypothesis is that the OB function is highly distributed, with that ability to perform odorant discriminations even with large lesions (Fecteau and Milgram, 2001). Recent studies consistent with this view, were done in transgenic zebra fish (Yaksi et al., 2004) and *Drosophila* antennal lobe (Wilson et al., 2004). They revealed that the selectivity of odorant preference given by the activated glomeruli input is substantially lost at the second order neuronal level, in addition to a coarser activation of these neurons. These findings are consistent with the idea that spatial organization observed at the glomeruli level, is at least, partially disrupted during olfactory coding at the MT cell level. One direct consequence of this transformation is the higher complexity of the response profiles of neighboring MT cells.

MT cells' oscillatory activity

Oscillations in the gamma-band are a robust event in LFP signals of the OB, and numerous studies have corroborated the its role in olfactory coding in vertebrates and invertebrates (Adrian, 1950; Gray and Skinner, 1988; Lam et al., 2000; Nusser et al., 2001; Perez-Orive et al., 2002; Ravel et al., 2003). To establish potential relationships between this rhythmic activity and MT cells firing properties, we assessed oscillatory properties of individual MT cells. Our results show that MT cells have no significant spontaneous oscillatory activity in the absence of odorants. The fact that single neurons showed no oscillatory firing patterns, while multi-unit recordings and local field

potentials do (Nusser et al., 2001; Ravel et al., 2003) indicates that LFP oscillations may arise from the sum of coordinated discharges of a given population. In other words, each MT cell contributes to the oscillatory cycles by firing in some of the cycles with precise timing within each of the cycles in which it fires (Laurent, 2002). This is coherent with the possibility of each MT cell having its own response properties, is able to participate in different ensembles not solely specified by their ORN inputs (Wilson et al., 2004).

Here we have shown that most of the MT cells exhibited a long silent period (~11 ms). Interestingly, this property remains during odorant presentation, suggesting that even under strong stimulation each MT cell may be exposed to inhibitory inputs that modulate its response to odorants. This particular feature is not always present in other sensory neurons (Friedman-Hill et al., 2000). Although further studies are needed to determine the origin of this long silent period, it likely arises from the reciprocal connectivity between MT cells and granular cells (Isaacson and Strowbridge, 1998). The reported gamma band of LFP oscillatory activity between 40 and 150 Hz (Buonviso et al., 2003; Ravel et al., 2003) is consistent with the 10 ± 5 ms silent periods observed in our single unit data and is congruent with the possibility of collective phase coherence as a mechanism that participates in olfactory coding at the output neurons in the OB.

Synchrony among neighboring MT cells

Neuronal synchrony in a millisecond time scale has been proposed as an integrative mechanism in which populations of encoding elements are formed (Singer and Gray, 1995). In our work, we analyzed synchronous activity among populations of neighboring MT cells. From the 58 cell pairs registered, only 2.8% of them showed synchronous activity during odorant stimulation. This result contrasts with that of Kashiwadani et al. (1999), where they reported that 27% of cell pairs examined in the dorsomedial region showed synchronous discharges. This study measured synchrony among MT cells that responded in a similar way to an odorant therefore their population of cells was selected. They also recorded from cells separated more than 300 μm and thus unlikely to be connected to the same glomerulus. Furthermore, differences in synchronous rates may be at least in part, due to the different criteria used to define synchronized activity. We employed a Monte-Carlo simulation with 99% cutoff value consistent with a stricter criterion than the one used by Kashiwadani et al. (1999). Finally, the use of artificial breathing may have affected the natural firing properties of the OB artificially yielding more synchrony. Our data demonstrate that although synchrony can be established among closely located pairs of neurons in the OB, this happens with a very low incidence. This is surprising considering that nearby neurons are likely to share ORN inputs. Indeed, recordings in OB slices showed that MT cells that synapse to the same glomerulus, show significantly more synchronous firing than those who synapse different glomeruli (Schoppa and Westbrook, 2002). Although our technique does not allow us to establish the synaptic organization of the MT cells recorded, the level of synchrony in neighboring cells that are presumably connected to the same glomerulus or at least to neighboring glomeruli suggests that other driving forces could influence the temporal behavior of MT cells. Furthermore, considering the low incidence of oscillatory behavior at the single from the underlying local rhythm, then the likelihood of joint firing between neighboring cells becomes significantly reduced.

Respiratory patterns among neighboring MT cells

Respiratory modulation of MT cells firing is a well-documented observation (Macrides and Chorover, 1972; Chaput et al., 1992). We found that these respiratory patterns are variable among neighboring MT cells. It is reasonable to think that firing patterns could be used as an encoding tool in the OB (Buonviso et al., 2003) and the observation that they appear to be individually modulated for each MT cell suggests than not only the odorant preferences are different from those giving by the ORN inputs, but the timing in which a cell fires is also modulated by the network within the OB. It is plausible to hypothesize that respiratory patterning contributes to odorant coding by endowing MT cells with a particular modulation during the respiratory cycle.

Conclusions

In this study we described the properties of populations of neighboring MT cells in anesthetized, freely breathing rats, while exposed to sets of chemically related compounds. The heterogeneity of temporal response properties and the molecular receptive range of neighboring MT cells presumably connected to the same or neighboring glomeruli indicate that the activity from ORNs is strongly modulated by interactions with other network elements within the OB. If we assume that MT cells connected to the same glomerulus form a functional module at the glomeruli level, our results suggest that the output of MT cells within this module is not necessarily identical. An advantage to this OB transformation of the ORN inputs is that heterogeneous groups of equally connected MT cells could work as decorrelators of odorant features to increase representation space (Laurent, 2002).

Acknowledgments—We thank Isaac Oporto for animal care and Bethany Snyder for comments on the manuscript. Supported by FONDECYT 1010811 CONICYT (JIE) and Iniciativa Científica Milenio ICM P01-007-F.

REFERENCES

Adrian ED (1950) The electrical activity of the mammalian olfactory bulb. Electroencephalogr Clin Neurophysiol 2:377–388.

Aungst JL, Heyward PM, Puche AC, Karnup SV, Hayar A, Szabo G, Shipley MT (2003) Centre-surround inhibition among olfactory bulb glomeruli. Nature 426:623–629.

Aylwin ML, Diaz E, Maldonado PE (2005) Simultaneous single unit recording in the mitral cell layer of the rat olfactory bulb under nasal and tracheal breathing. Biol Res, in press.

Belluscio L, Katz LC (2001) Symmetry, stereotypy, and topography of odorant representations in mouse olfactory bulbs. J Neurosci 21:2113–2122.

Buck L, Axel R (1991) A novel multigene family may encode odorant receptors: a molecular-basis for odor recognition. Cell 65:175–187.

Buck LB (2000) The molecular architecture of odor and pheromone sensing in mammals. Cell 100:611–618.

Buonviso N, Amat C, Litaudon P, Roux S, Royet JP, Farget V, Sicard G (2003) Rhythm sequence through the olfactory bulb layers during the time window of a respiratory cycle. Eur J Neurosci 17:1811–1819.

Buonviso N, Chaput MA (1990) Response similarity to odors in olfactory bulb output cells presumed to be connected to the same glomerulus: electrophysiological study using simultaneous single-unit recordings. J Neurophysiol 63:447–454.

Buonviso N, Chaput MA, Berthommier F (1992) Temporal pattern analyses in pairs of neighboring mitral cells. J Neurophysiol 68:417–424.

Buonviso N, Chaput MA, Scott JW (1991) Mitral cell-to-glomerulus connectivity: an HRP study of the orientation of mitral cell apical dendrites. J Comp Neurol 307:57–64.

Buzsaki G (2004) Large-scale recording of neuronal ensembles. Nat Neurosci 7:446–451.

Chalansonnet M, Chaput MA (1998) Olfactory bulb output cell temporal response patterns to increasing odor concentrations in freely breathing rats. Chem Senses 23:1–9.

Chaput MA (1986) Respiratory-phase-related coding of olfactory information in the olfactory bulb of awake freely-breathing rabbits. Physiol Behav 36:319–324.

Chaput MA, Buonviso N, Berthommier F (1992) Temporal patterns in spontaneous and odor-evoked mitral cell discharges recorded in anesthetized freely breathing animals. Eur J Neurosci 4:813–822.

Christie JM, Westbrook GL (2003) Regulation of backpropagating action potentials in mitral cell lateral dendrites by A-type potassium currents. J Neurophysiol 89:2466–2472.

Fecteau J, Milgram NW (2001) The ability to smell remains intact, but does not recover, after olfactory bulb lesions. Int J Neurosci 108:11–20.

Firestein S (2001) How the olfactory system makes sense of scents. Nature 413:211–218.

Fried HU, Fuss SH, Korsching SI (2002) Selective imaging of presynaptic activity in the mouse olfactory bulb shows concentration and structure dependence of odor responses in identified glomeruli. Proc Natl Acad Sci U S A 99:3222–3227.

Friedman-Hill S, Maldonado PE, Gray CM (2000) Dynamics of striate cortical activity in the alert macaque: I. Incidence and stimulus-dependence of gamma-band neuronal oscillations. Cereb Cortex 10:1105–1116.

Friedrich RW, Laurent G (2001) Dynamic optimization of odor representations by slow temporal patterning of mitral cell activity. Science 291:889–894.

Gray CM, Maldonado PE, Wilson M, McNaughton B (1995) Tetrodes markedly improve the reliability and yield of multiple single-unit isolation from multi-unit recordings in cat striate cortex. J Neurosci Methods 63:43–54.

Gray CM, Skinner JE (1988) Centrifugal regulation of neuronal activity in the olfactory bulb of the waking rabbit as revealed by reversible cryogenic blockade. Exp Brain Res 69:378–386.

Gray CM, Viana DP (1997) Stimulus-dependent neuronal oscillations and local synchronization in striate cortex of the alert cat. J Neurosci 17:3239–3253.

Inaki K, Takahashi YK, Nagayama S, Mori K (2002) Molecular-feature domains with posterodorsal-anteroventral polarity in the symmetrical sensory maps of the mouse olfactory bulb: mapping of odourant-induced Zif268 expression. Eur J Neurosci 15:1563–1574.

Isaacson JS, Strowbridge BW (1998) Olfactory reciprocal synapses: dendritic signaling in the CNS. Neuron 20:749–761.

Jahr CE, Nicoll RA (1980) Dendrodendritic inhibition: demonstration with intracellular recording. Science 207:1473–1475.

Johnson BA, Ho SL, Xu Z, Yihan JS, Yip S, Hingco EE, Leon M (2002) Functional mapping of the rat olfactory bulb using diverse odorants reveals modular responses to functional groups and hydrocarbon structural features. J Comp Neurol 449:180–194.

Johnson BA, Leon M (2000) Modular representations of odorants in the glomerular layer of the rat olfactory bulb and the effects of stimulus concentration. J Comp Neurol 422:496–509.

Johnson BA, Woo CC, Leon M (1998) Spatial coding of odorant features in the glomerular layer of the rat olfactory bulb. J Comp Neurol 393:457–471.

Kashiwadani H, Sasaki YF, Uchida N, Mori K (1999) Synchronized oscillatory discharges of mitral/tufted cells with different molecular receptive ranges in the rabbit olfactory bulb. J Neurophysiol 82:1786–1792.

Kay LM, Laurent G (1999) Odor- and context-dependent modulation of mitral cell activity in behaving rats. Nat Neurosci 2:1003–1009.

Kishi K, Mori K, Ojima H (1984) Distribution of local axon collaterals of mitral, displaced mitral, and tufted cells in the rabbit olfactory bulb. J Comp Neurol 225:511–526.

Lam YW, Cohen LB, Wachowiak M, Zochowski MR (2000) Odors elicit three different oscillations in the turtle olfactory bulb. J Neurosci 20:749–762.

Laurent G (1996) Dynamical representation of odors by oscillating and evolving neural assemblies. Trends Neurosci 19:489–496.

Laurent G (1999) A systems perspective on early olfactory coding. Science 286:723–728.

Laurent G (2002) Olfactory network dynamics and the coding of multidimensional signals. Nat Rev Neurosci 3:884–895.

Macrides F, Chorover SL (1972) Olfactory bulb units: activity correlated with inhalation cycles and odor quality. Science 175:84–87.

Macrides F, Schneider SP (1982) Laminar organization of mitral and tufted cells in the main olfactory bulb of the adult hamster. J Comp Neurol 208:419–430.

Maldonado PE, Friedman-Hill S, Gray CM (2000) Dynamics of striate cortical activity in the alert macaque: II. Fast time scale synchronization. Cereb Cortex 10:1117–1131.

Maldonado PE, Gray CM (1996) Heterogeneity in local distributions of orientation-selective neurons in the cat primary visual cortex. Vis Neurosci 13:509–516.

Margrie TW, Sakmann B, Urban NN (2001) Action potential propagation in mitral cell lateral dendrites is decremental and controls recurrent and lateral inhibition in the mammalian olfactory bulb. Proc Natl Acad Sci U S A 98:319–324.

Meister M, Bonhoeffer T (2001) Tuning and topography in an odor map on the rat olfactory bulb. J Neurosci 21:1351–1360.

Mombaerts P, Wang F, Dulac C, Vassar R, Chao SK, Nemes A, Mendelsohn M, Edmondson J, Axel R (1996) The molecular biology of olfactory perception. Cold Spring Harb Symp Quant Biol 61:135–145.

Mori K, Kishi K, Ojima H (1983) Distribution of dendrites of mitral, displaced mitral, tufted, and granule cells in the rabbit olfactory bulb. J Comp Neurol 219:339–355.

Mori K, Mataga N, Imamura K (1992) Differential specificities of single mitral cells in rabbit olfactory bulb for a homologous series of fatty acid odor mulecules. J Neurophysiol 67:786–789.

Nagayama S, Takahashi YK, Yoshihara Y, Mori K (2004) Mitral and tufted cells differ in the decoding manner of odor maps in the rat olfactory bulb. J Neurophysiol 91:2532–2540.

Nusser Z, Kay LM, Laurent G, Homanics GE, Mody I (2001) Disruption of GABA(A) receptors on GABAergic interneurons leads to increased oscillatory power in the olfactory bulb network. J Neurophysiol 86:2823–2833.

Orona E, Scott JW, Rainer EC (1983) Different granule cell populations innervate superficial and deep regions of the external plexiform layer in rat olfactory bulb. J Comp Neurol 217:227–237.

Perez-Orive J, Mazor O, Turner GC, Cassenaer S, Wilson RI, Laurent G (2002) Oscillations and sparsening of odor representations in the mushroom body. Science 297:359–365.

Ravel N, Chabaud P, Martin C, Gaveau V, Hugues E, Tallon-Baudry C, Bertrand O, Gervais R (2003) Olfactory learning modifies the expression of odour-induced oscillatory responses in the gamma (60–90 Hz) and beta (15–40 Hz) bands in the rat olfactory bulb. Eur J Neurosci 17:350–358.

Ressler KJ, Sullivan SL, Buck LB (1994) Information coding in the olfactory system: evidence for a stereotyped and highly organized epitope map in the olfactory bulb. Cell 79:1245–1255.

Rubin BD, Katz LC (1999) Optical imaging of odorant representations in the mammalian olfactory bulb. Neuron 23:499–511.

Rubin BD, Katz LC (2001) Spatial coding of enantiomers in the rat olfactory bulb. Nat Neurosci 4:355–356.

Schoppa NE, Kinzie JM, Sahara Y, Segerson TP, Westbrook GL (1998) Dendrodendritic inhibition in the olfactory bulb is driven by NMDA receptors. J Neurosci 18:6790–6802.

Schoppa NE, Urban NN (2003) Dendritic processing within olfactory bulb circuits. Trends Neurosci 26:501–506.

Schoppa NE, Westbrook GL (2001) Glomerulus-specific synchronization of mitral cells in the olfactory bulb. Neuron 31:639–651.

Schoppa NE, Westbrook GL (2002) AMPA autoreceptors drive correlated spiking in olfactory bulb glomeruli. Nat Neurosci 5:1194–1202.

Shipley MT, Ennis M (1996) Functional organization of olfactory system. J Neurobiol 30:123–176.

Singer W, Gray CM (1995) Visual feature integration and the temporal correlation hypothesis. Annu Rev Neurosci 18:555–586.

Tabor R, Yaksi E, Weislogel JM, Friedrich RW (2004) Processing of odor mixtures in the zebrafish olfactory bulb. J Neurosci 24:6611–6620.

Uchida N, Mainen ZF (2003) Speed and accuracy of olfactory discrimination in the rat. Nat Neurosci 6:1224–1229.

Uchida N, Takahashi YK, Tanifuji M, Mori K (2000) Odor maps in the mammalian olfactory bulb: domain organization and odorant structural features. Nat Neurosci 3:1035–1043.

Vassar R, Chao SK, Sitcheran R, Nunez JM, Vosshall LB, Axel R (1994) Topographic organization of sensory projections to the olfactory bulb. Cell 79:981–991.

Wilson RI, Turner GC, Laurent G (2004) Transformation of olfactory representations in the Drosophila antennal lobe. Science 303: 366–370.

Xiong W, Chen WR (2002) Dynamic gating of spike propagation in the mitral cell lateral dendrites. Neuron 34:115–126.

Yaksi E, Higashijima S, Mandel G, Fetcho J, Firedrich R (2004) Chemotopy in the zebrafish olfactory system studied with a transgenic calcium indicator. Program No. 531.13.2004 Abstract Viewer/Itinerary Planner. Washington, DC: Society for Neuroscience.

Zou Z, Horowitz LF, Montmayeur JP, Snapper S, Buck LB (2001) Genetic tracing reveals a stereotyped sensory map in the olfactory cortex. Nature 414:173–179.